Heliyon 10 (2024) e33033

Contents lists available at ScienceDirect

Heliyon

journal homepage: www.cell.com/heliyon

Research article

Prognosis recovery score of apical surgery Guided Bone Regeneration using cone beam computed tomography and digital bioinformatics

Pablo Rodríguez [a], Isabel Adler [a], María Lorena Cabirta [a], Eugenia Miklaszewski [a], Nicolás Alfie [a], Andrea Muiño [a], Sara Chulián [b], Cristóbal Fresno [c,1], Valeria Denninghoff [d,e,*,1]

[a] Faculty of Dentistry, University of Buenos Aires (UBA), Argentina
[b] Andalusian Public Foundation Progress and Health - Andalusian Regional Government (FPS), Sevilla, Spain
[c] Health Sciences Research Center (CICSA), Anáhuac University Mexico, Mexico
[d] Molecular-Clinical Lab–University of Buenos Aires (UBA) - National Council for Scientific and Technical Research (CONICET), Argentina
[e] Liquid Biopsy and Cancer Interception Group, Centre for Genomics and Oncological Research–Pfizer–University of Granada - Andalusian Regional Government (GENyO), Granada, Spain

ARTICLE INFO

Keywords:
Bone graft(s)
Bone remodeling/regeneration
Computed tomography
Dental informatics/bioinformatics
Digital imaging/radiology

ABSTRACT

Objective: Guided Bone Regeneration (GBR) is a dental surgical procedure that uses barrier membranes to prevent soft tissue invasion and conduct new bone growth. This study aimed to define a Prognosis Recovery score (PR score) to objectively classify post-surgery responders from non-responder patients who underwent GBR using Cone Beam Computed Tomography (CBCT).
Methods: This prospective-observational-longitudinal-cohort study recruited 250 individuals who were assigned to: Conventional-Apical-Surgery (CAS, n = 39), Apical-Surgery using human fascia lata Membrane placement (ASM, n = 42), and Apical-Surgery using human fascia lata Membrane placement and lyophilized allograft Bone powder (ASMB, n = 39); and Apical-Surgery using collagen membrane Porcine origin and Bovine Bone-matrix (ASPBB, n = 130), an independent external validation cohort. Surgery was performed, and evolution was monitored by CBCTs at 0, 6-, 12-, 18-, and 24 months post-surgery.
Results: Normalized lesion volumes were calculated, and non-linear time evolution morphology curves were characterized. The three-time evolution bone growth patterns were: a linear tendency (PR0), "S'' shaped log-logistic (PR1), and "C" cellular growth (PR2). The treatment success rates were PR2-46 %, PR2-88 %, and PR2-95 %/PR1-5% for CAS, ASM, and ASMB groups. The xenograft ASPBB counterpart achieved PR2-92 % and PR1-8%. The score PR had a sensitivity, specificity, and accuracy of 100 %.
Conclusions: Patients' treatment success can be quantitatively, objectively, and precisely predicted with the Prognosis Recovery score (using only two CBCTs), according to their biological response to allograft or xenograft materials (time-evolution bone growth curves), reducing cost and radiation exposure.

* Corresponding author. University of Buenos Aires (UBA), Marcelo Torcuato de Alvear 2142, C1122AAH, Buenos Aires, Argentina.
E-mail address: vdenninghoff@conicet.gov.ar (V. Denninghoff).
[1] These authors contributed equally to this work.

https://doi.org/10.1016/j.heliyon.2024.e33033
Received 3 January 2024; Received in revised form 12 June 2024; Accepted 13 June 2024
Available online 15 June 2024

Clinical significance: Through digital imaging and bioinformatic analysis of bone regeneration observed in CBCTs, we defined a Prognosis Recovery (PR) score using only two CBCT volume assessments (0 and 6 months). The PR score allowed us to define three time-evolution curves depending on the biomaterials used and to classify patients in a quantitative, objective, and accurate way.

1. Introduction

Guided Bone Regeneration (GBR) is a dental surgical procedure that uses barrier membranes to prevent soft tissue invasion and conduct new bone growth for proper function, esthetics, or implant therapy [1,2]. Membranes with barrier function have been shown to achieve good results and, together with bone graft material, to speed up the recovery time through osteogenesis, osteoinduction, and osteoconduction [3–5]. Biocompatibility and osteoinductivity, without an antigenic effect, are vital clinical requirements for bone materials.

There are four options for bone graft material. Autologous/autogenous bone is the "gold standard" among graft materials because its solid osteogenic characteristics are relevant to bone healing, modeling, and remodeling [6]. Non-essential bones of the same individual constitute the first choice for autologous bone grafting. Allograft biomaterial is a valid second option, i.e., tissue transferred from one individual to a genetically different one belonging to the same species, obtained from cadaveric material or a bone bank. Allograft bone's main benefit is avoiding a secondary donor site, reducing surgical time, decreasing blood loss, decreasing host morbidity, and having an unlimited supply of graft material [7]. The third alternative is using bone substitutes for xenografts - tissue donors of other species such as bovine or porcine. Depending on the origin, xenografts could carry a risk of transmission of zoonotic diseases; thus, graft rejection would be more likely and aggressive [8]. Both allografts and xenografts need to eliminate antigenicity by freeze-drying, demineralizing, and deproteinizing treatments [7]. Although they conserved osteoinductive and osteoconductive characteristics, they lack the osteogenic properties of autologous grafts; therefore, bone generation usually takes longer [7,8]. Bovine xenograft showed a better biological response than the other bone graft substitutes; however, more clinical studies are necessary to determine its effectiveness [9]. The last option is alloplastic grafts, which are synthetic, inorganic, and biocompatible bone substitutes that work as fillers to repair skeletal defects [10].

Cone Beam Computed Tomography (CBCT) measures post-surgical follow-up. CBCT is more sensitive than conventional radiography in detecting apical periodontitis and assessing osseous healing [11]. The benefit of using a CBCT is to measure the volume of the actual initial apical process and the 3D evolution of the repair of the lesion over time (image 1:1) [12]. Treatment success is usually determined at 12 or 24 months by CBCT, without inferred biomedical results or prognoses during that window of time. Therefore, it would be necessary to objectively evaluate patients with images within the inter periods from 0 to 24 months. No literature has quantitatively and objectively evaluated the response of GBR. Therefore, GBR requires a predictive factor of bone regeneration, defined as any measurement associated with the response to a given treatment that identifies subgroups of treated patients with different outcomes due to therapy.

2. Objectives

The study's main objective is to describe a prognostic factor that allows us to estimate bone formation after apical surgery-GBR. The secondary objectives of this study were.

- To quantitatively and objectively measure the reduction of the boneless maxillary area determined by bone neoformation over time, using CBCT post-surgical (time 0) and over 6, 12, 18, and 24 months in patients after apical surgery-GBR.
- To objectively compare the efficacy of the treatments used in an apical surgery-GBR by constructing time-evolution curves and confirm that the membrane added to the apical surgery-GBR accelerates bone neoformation in the time-evolution curve.
- To design a score using CBCT and digital bioinformatics to differentiate responders from non-responders and validate the designed score for a different population.

3. Materials and methods

3.1. Study cohort

This prospective-observational-longitudinal-cohort study recruited all patients who attended the Endodontics Chair of a Public Hospital of the Central University in 2011, diagnosed using a preoperative digital x-ray and a clinical evaluation at the Endodontic Microsurgery Service (Fig. 1). The inclusion criteria were: Patients over 18 years old, who presented teeth with the necessity of Apical Surgery, with radiographic periapical lesion involving at least two teeth that showed: a) Endodontic treatment, with persistence or appearance of the periapical lesion and clinical symptoms; b) Poor root canal treatment, periapical lesions, and clinical symptoms; and c) Periapical lesions and clinical manifestations that presented post-endodontic reconstruction with rigid root anchorage and which removal would put root integrity at risk. The exclusion criteria were the absence of a signature on the informed consent, smokers,

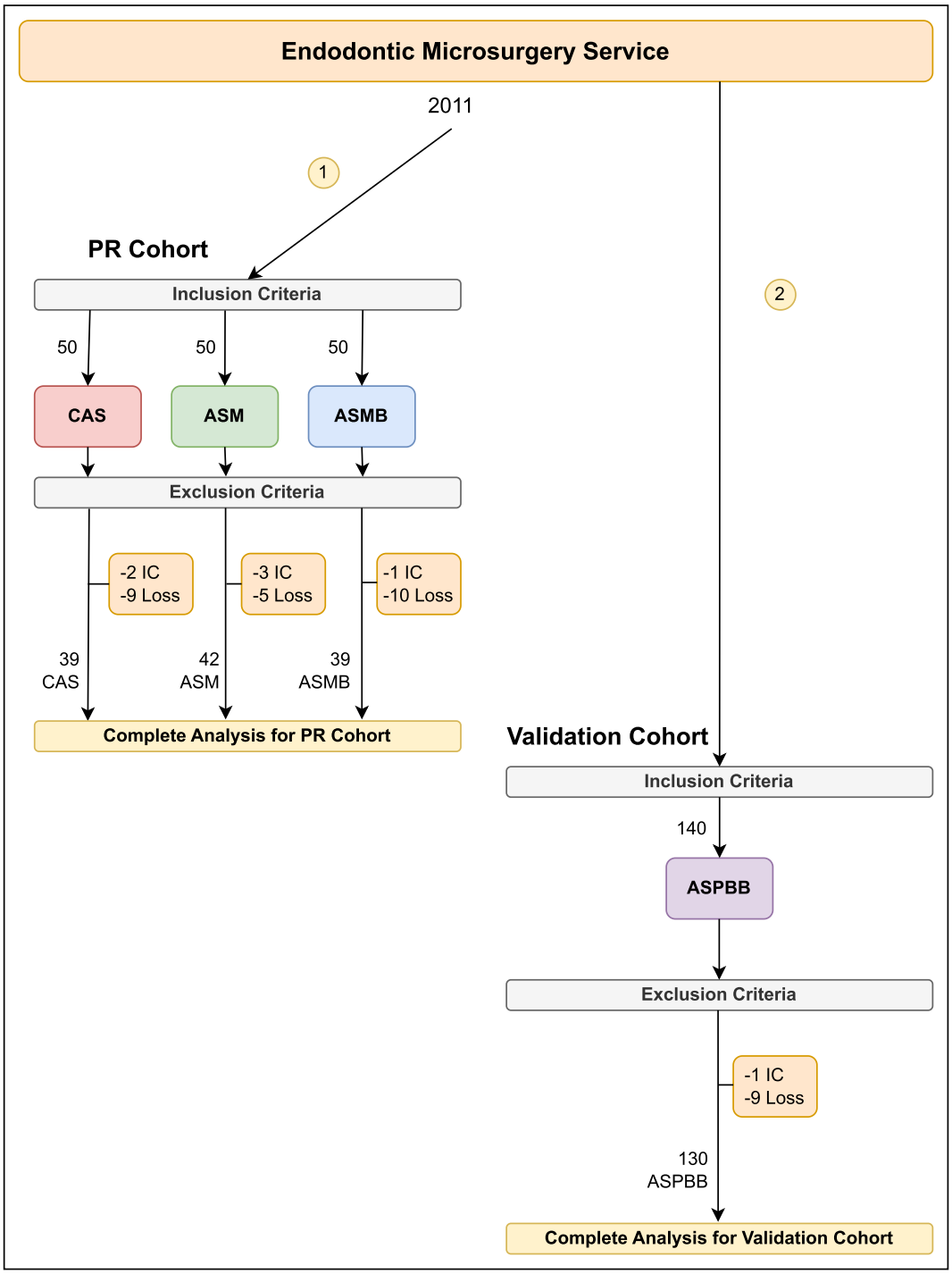

Fig. 1. Study Flow Diagram
PR: Prognosis Recovery; CAS: Conventional Apical Surgery; ASM: Apical Surgery with human fascia lata Membrane placement; ASMB: Apical Surgery human fascia lata Membrane placement and lyophilized allograft Bone powder; ASPBB: Apical Surgery with Porcine membrane and Bovine Bone; IC: not signed Informed Consent; Loss: Follow-up lost.

history of drug abuse, pre-existing systemic pathologies, any current antibiotic treatment, patients with periapical lesions involving less than two teeth, lack of any of the four follow-up CBCTs, and loss of follow-up.

The study was conducted according to the guidelines of the Declaration of Helsinki, and the Ethics Commission approved it. On the other hand, the Central National Institute Coordinator for Ablation and Implant (INCUCAI) approved using human-biobank membrane and bone materials (allografts).

The first 150 patients were recruited to measure bone neoformation over time, design a score, and construct time-evolution curves with different allograft biomaterial combinations (PR cohort, Fig. 1). They were distributed as they were recruited into the three groups, one by one, ensuring the study's unbiased nature (50 in each group).

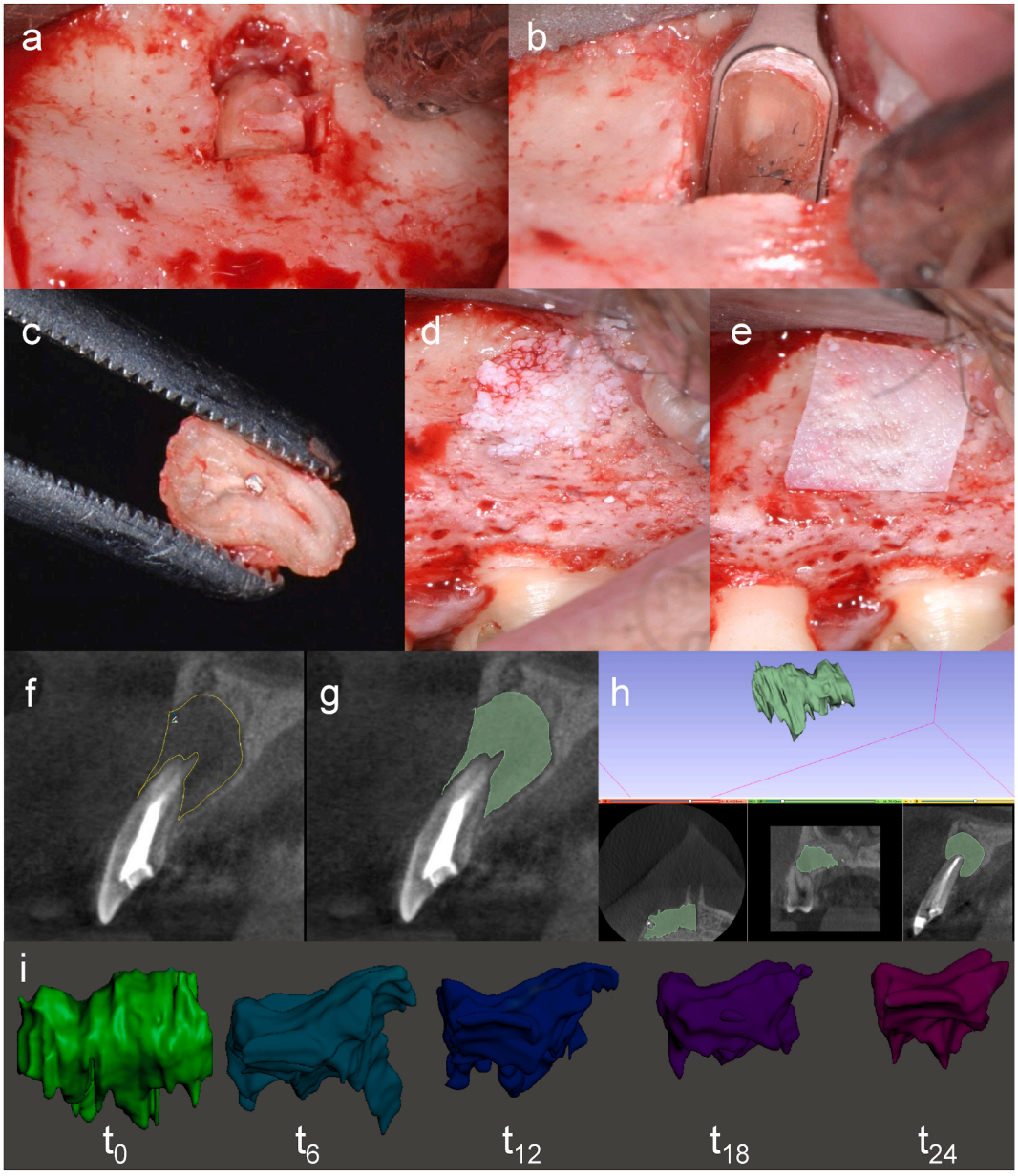

Fig. 2. The apical surgery procedure with placement of fascia lata membrane and lyophilized homologous bone powder. (a) Apical 3 mm osteotomy and dissection. (b) The remaining root was sectioned, and (c) sectioned apex. (d) Bone substitute placement. (e) Membrane placement. (f) The initial Cone-Beam Computed Tomography was used to set the lesion border limit (green border), (g) to estimate the lesion area with a lesion segmentation process in a sagittal view depicted in green, and complete lesion volume assessment, using a composition image with multiplanar and three-dimensional visualization of the lesion using additional angles (3D Slicer v4.11). (h) Three-dimensional visualization of the lesion that (i) estimated volume evolution at 0, 6, 12, 18, and 24 months (Autodesk Meshmixer). (For interpretation of the references to color in this figure legend, the reader is referred to the Web version of this article.)

- Conventional-Apical-Surgery (CAS)
- Apical-Surgery using human fascia lata Membrane placement (ASM)
- Apical-Surgery using human fascia lata Membrane placement and lyophilized allograft Bone powder (ASMB).

Once the 150 patients were completed, the others recruited during the year would be included to validate the designed score in a different, independent external population with xenograft biomaterial and to calculate sensitivity and specificity (validation cohort, Fig. 1).

- Apical-Surgery using collagen membrane Porcine origin and Bovine Bone-matrix (ASPBB).

3.2. Surgical procedure

The surgery was performed under infiltrative anesthesia, making an intrasulcular incision at the level of the compromised pieces rising a Neumann flap (trapezoidal or triangular) followed by mucoperiosteal flap cleavage (of the total thickness, Fig. 2a–e). Osteotomy was performed with a piezoelectric scalpel (Variosurg, NSK, Osaka, Japan) with constant irrigation with a sterile physiological solution [13]. The peri-radicular lesion removal was performed with microsurgery curettes, then proceeded with two applications of 20 s of intra-cavitary placement of hydrochloride tetracycline powder diluted in distilled water, later washed with a physiological solution to use its acidic pH to degrade the organic tissue and facilitate the removal of adhered fibrous tissue [14]. The bone margins were regularized. The root-end resection was performed with ultrasonic diamond tips generating a vestibular bezel from zero to ten degrees, with a length of not less than 3 mm from the anatomical root end [13]. Subsequently, the preparation was done, again with ultrasonic tips, followed by root-end filling with a bio-ceramic sealer (Bio C Sealer, Londrina, PR, Brazil). According to the assigned group, different biomaterials were used: ASM: lyophilized collagen resorbable membrane (Ostium Fascia Lata-L); ASMB: lyophilized collagen resorbable membrane (Ostium Fascia Lata-L) plus lyophilized ground spongy bone matrix implant (Ostium); and ASPBB: bovine bone matrix implant (OstiumMax) plus collagen porcine origin membrane (OstiumMax Cover). Finally, the flaps were repositioned without tension with a nylon thread suture (five or six zeros) for all groups. The patient's postoperative treatment was Amoxicillin 500 mg/8 h for seven days, Ibuprofen 400 mg/8 h for four days, and Chlorhexidine Di gluconate 0.12 % by topical application gel on the wound [14].

3.3. Guided bone recovery characterization

CBCTs monitored evolution at 0, 6-, 12-, 18-, and 24 months post-surgery to characterize the tissue growth for both cohorts (Fig. 2f–i). The equipment used was a Radiovisiograph/RVG/Digital sensor (Kodak 2100 & 2200 Intraoral X-ray Systems) and a CBCT Scanner (Kodak, 9000C 3D). The CBCT scans were performed at a voltage of 96 kV, a current of 9 mA, and an exposure time of 15 s, selecting a FoV reduced to 3.7 cm high and 5 cm wide, reaching a voxel size of 75 μm. Tomographic images used DICOM (single frame) 16-bit deep tiff format. A single operator did all interventions with an operating optical microscope (Opmi Pico, Karl Zeiss, Germany).

3.4. Digital imaging analysis

We used the 3D Slicer Software v4.11.202110226 to visualize and measure bone lesions by CBCT, used the segment editor module with manual, semi-automatic, and automatic tools for image segmentation, and used the segment statistics module to calculate the area and volume of the selected segments (https://www.slicer.org). Tissue density was evaluated in gray value units, obtaining a minimum density value for the mineralized tissue, but without discriminating between bone grafts or new bone tissue. Once a compliant result was obtained, the volume was measured in mm^3.

3.5. Treatment outcome

The absolute lesion volume (V) over time (t) was called Vt and was estimated using CBCT biomedical imaging analysis. To compare lesion volume evolution for each patient, we normalized the volume using the first-time measurement ($t = 0$) as a reference. Hence, the Percentage (P) volume for each time (PVt) was calculated by $PVt = Vt/V0 \times 100$ %. The apical surgery-GBR treatment was considered a success if the $PV24 < 25$ %, i.e., responder patients had a residual percentage volume lower than 24 % at 24 months. On the contrary, treatment failure (non-responder) required a $PV24 \geq 25$ %.

3.6. Prognosis recovery score

Provided that the PVt is an un-biased normalization which will allow us to compare the lesion recovery of the patients over time, here, we propose a prognosis recovery score with the following aspects: i) predict apical surgery-GBR treatment success at the earliest as possible (6 months); ii) be categorized into to three mutually exclusive classes (PR0, PR1, and PR2); and iii) be ordinal in the sense that the treatment response chances can be increasing, i.e., $PR0 \leq PR1 \leq PR2$. Formally, we define the PR score as follows.

- PR0: if PV6 $>$ 75 %, i.e., treatment failure.
- PR1: if 75 % $\geq$ PV6 $\geq$ 50 %, i. e., surveillance at 12 months post-surgery.
- PR2: if PV6 $<$ 50 % i. e., treatment success.

3.7. Bone neoformation time-evolution

The time-evolution of the different PR scores (PR0, PR1, and PR2) can be characterize using the PVt into three different patterns as linear tendencies, “S" or “C"-shaped curves as described below.

■ Linear Tendency

The rationale behind this pattern is to model data with a limited biological response, where the PVt fails to reduce over time, resulting in a slight lesion reduction. Formally, a linear mixed-effect model can be used to address this task through equation Eq. (1):

$$y_{ijkl} = \mu + \alpha_i + \beta_j + a_k + b_l + \varepsilon_{ijkl} \tag{1}$$

where.

- y_{ijkl} was the observed percentage volume for the i-th time at the j-th treatment, for the k-th sex of the l-th patient.
- μ was the population global percentage volume intercept.
- α_i was the i-th time fixed effect.
- β_j was the j-th treatment fixed effect (if present).
- $a_k \sim N(0, I\sigma_G^2)$ was the random intercept for the k-th sex level (male or female).
- $b_l \sim N(0, I\sigma_P^2)$ was the random intercept for the l-th patient level.
- $\varepsilon_{ijkl} \sim N(0, I\sigma_\varepsilon^2)$ was the random error term for the given sample.

■ “C”-shaped curveProbably is the most biological expected population cellular growth pattern, which resembles a typical “C”-shaped curve, where expressed the standard formulation in a decreasing manner, as depicted in equation Eq. (2):

$$y = 100 - \left[a + (b - a) \times e^{-e^c \times Time}\right] \tag{2}$$

where.

- y was the observed percentage volume.
- a was the lower asymptote.
- b was the higher asymptote.
- c was the halfway response between a and b asymptotes.

■ “S”-shaped curveIf the patients react to the apical microsurgery, it has a slow osteocyte growth followed by a sudden fast response, resembling an “S” shaped curve. This pattern had long been modeled in biology by a log-logistic regression according to equation Eq. (3):

$$y = a + \frac{c - a}{1 + e^{b \times [log\ (Time)\ - log\ (d)\ ]}} \tag{3}$$

where.

- y was the observed percentage volume.
- a was the lower asymptote.
- b was the decreasing slope.
- c was the higher asymptote.
- d was the halfway response between a and c asymptotes.

Model of Eq. (1) can be fitted using the lme4 R package, whereas models of Eqs. (2) and (3)require non-linear least squares models of the types that the nlme R package can implement [15,16]. For models of Eqs. (2) and (3), the fixed coefficient contribution was modeled as $a + b + c \sim 1 + Treatment$ to explore if the treatment contribution exists in each parameter. In addition, the random formula was expressed as $a + b + c \sim 1$, i.e., every coefficient had the same random structure.

Companion analysis of the variance tables from the car R package can be created with the appropriate type III sum of squares to evaluate model results and perform the model selection by maximum likelihood strategy [15].

3.8. Statistical analysis

We conducted all analyses using the R language. Univariate descriptive statistics included mean and standard deviation calculations for numerical data (age and lesion volume), as well as contingency tables for categorical data (sex assigned at birth, dental location, and treatment outcome). Group assignment bias was tested by analysis of the variance and $\chi 2$ tests for numeric or categorical variables, respectively. Successful treatment proportions were estimated using a binomial 95 % confidence interval (CI 95 %). Multivariate bone-tissue time evolution growth patterns were modeled using a linear mixed-effect model or non-linear regression and compared by maximum-likelihood test. Except where noted, all statistical tests were two-sided with a $p < 0.05$ for statistical significance.

4. Results

The PR cohort was CAS n = 39, ASM n = 42, and ASMB n = 39. The Validation cohort was ASPBB n = 130 (Fig. 1). In both cohorts, the patients lost were due to patients who did not sign the informed consent or without follow-up. Among the patients with complete data, the sex (p = 0.57), age (p = 0.22), and location (p = 0.26) did not have significant differences between the treatment levels (CAS, ASM, ASMB, or ASPBB) (Table 1). When treated as independent variables to model age, there was no association between treatment (p = 0.22) and sex (p = 0.12).

4.1. Time-evolution biomaterial-dependent patterns

We performed a temporal analysis of the bone neoformation (residual lesion volume) to compare the graft's bone formation quantitatively due (Fig. 3a). This approach allowed us to characterize different patterns as linear tendencies, "S" or "C"-shaped curves.

The linear tendency included 54 % of the CAS and 12 % of ASM group patients and had a similar behavior 99.82 %–0.61 % x Time no matter the treatment (Table 2). This line ended at PV24 > 70 %, indicating a clear treatment failure. On the other hand, two ASMB patients (5 %, Table 2) followed a log-logistic "S" shaped curve. This pattern showed a delay at the beginning of the osteocyte's growth, which departed its behavior from PR0 (linear tendency) and rapidly recovered after 12 months, reaching a PV24 < 25 %, indicative of treatment success. Finally, there is a "C" shaped cellular growth pattern, as expected by the literature. To the best of our knowledge,

Table 1
Characteristics of the study population according to the graft biomaterial used.

	CAS	ASM	ASMB	ASPBB
Sex [n]				
p-value = 0.57				
Total	39	42	39	130
Male	24	21	21	55
Female	15	21	18	75
Age [years±SD]]				
Biomaterial p-value = 0.22,				
Gender p-value = 0.12				
Total	37 ± 12	40 ± 15	43 ± 15	47 ± 17
Male	38 ± 12	36 ± 15	41 ± 16	46 ± 17
Female	36 ± 13	45 ± 14	45 ± 3	47 ± 17
Dental Location [n]]				
p-value = 0.26				
Total	39	42	39	130
Right	35	34	36	71
Left	4	8	3	59
Outcome [n]]				
p-value = 0.72				
Total|M|F	39|24|15	42|21|21	39|21|18	130|55|75
Success(%)|M|F	18(46)|14|4	37(**88**)|18|19	39(**100**)|21|18	130(**100**)|55|75
Failure(%)|M|F	21(**54**)|10|11	5|3|2	0|0|0	0|0|0
Residual Volume [%±SD]]				
Initial	100 ± 0.0	100 ± 0.0	100 ± 0.0	100 ± 0.0
6 Months	**67.1 ± 32.0**	**38.8 ± 22.6**	**20.6 ± 2.3**	**16.3 ± 15.0**
12 Months	58.0 ± 38.3	20.7 ± 27.8	11.6 ± 6.4	3.9 ± 7.7
18 Months	51.2 ± 41.4	15.9 ± 28.3	7.3 ± 4.7	1.0 ± 2.5
24 Months	46.5 ± 41.9	11.9 ± 28.1	3.0 ± 2.7	0.2 ± 0.7

CAS.: Conventional Apical Surgery; ASM.: Apical Surgery with human fascia lata Membrane placement; ASMB.: Apical Surgery human fascia lata Membrane placement and lyophilized allograft Bone powder; ASPBB.: Apical Surgery with Porcine membrane and Bovine Bone; n: number of individuals; SD.: Standard Deviation; %: perceptual value; M: Male and F: Female. Categorical variables were tested using a χ^2 test. Age was tested using a two-way Analysis of the Variance (ANOVA) for the study population and gender, respectively. ANOVA assumptions for the residual volume were not satisfied.

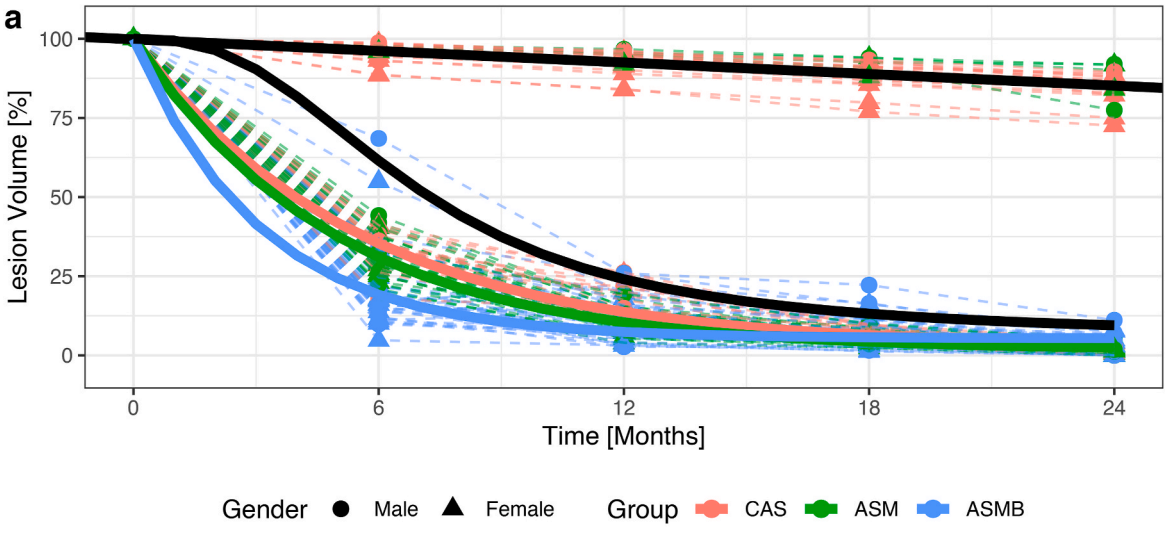

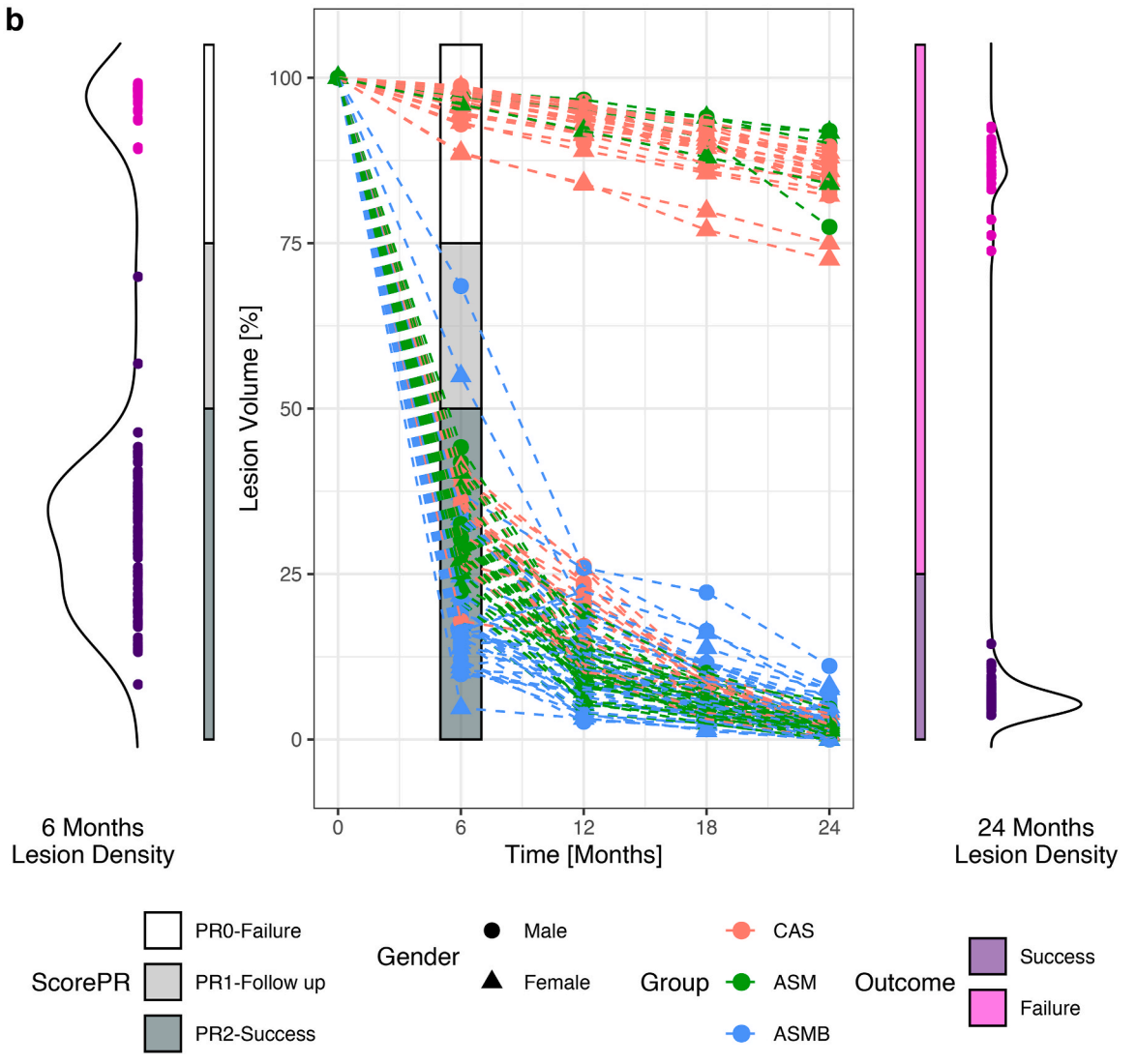

(caption on next page)

Fig. 3. Guided Bone Regeneration Predictive Recovery score (PR score) development. (a) The lesion time evolution was fitted according to the experimental group (continuous line). A linear decreasing growth (in black), where there is no difference between treatments (CAS and ASM) group according to the Type III Wald $\chi 2$ tests (p-value = 0.23). An "S" shaped log-logistic curve (in black), whereas the remaining treatments had a lesion volume reduction following a non-linear "C" shaped cellular growth tendency. (b) The lesion volume time evolution of the three treatments (CAS, ASM, or ASMB) can be seen at 0, 6, 12, 18, and 24 months. At the 24-month mark, distinct bimodal density patterns (represented by right density curves) emerge for failure (magenta) and success (purple) data points. These colored data points facilitate a binary partition of the injury space, delineated by magenta and purple rectangles. A similar bimodal behavior is observable at six months, with the injury time point (depicted in the left density plot) exhibiting the same pattern. In this analysis, outcome color-coding is employed to associate outcomes with the respective density curves. The lesion space is then categorized into three scores—PR0 for Failure, PR1 for Follow-up, and PR2 for Success—corresponding to the white, ivory, and gray-filled rectangles, respectively.
CAS: Conventional Apical Surgery; ASM: Apical Surgery with human fascia lata Membrane placement; ASMB: Apical Surgery human fascia lata Membrane placement and lyophilized allograft Bone powder. The lesion space is categorized into three scores —PR0 for failure, PR1 for follow-up, and PR2 for success. PR0 was modeled using linear decreasing growth; PR1 was modeled using an "S" shaped log-logistic curve $y = a + \frac{c-a}{1+e^{b\times[log\ (Time)\ -log\ (d)]}}$; PR2 was modeled using a "C" shaped cellular growth tendency $y = 100 - \left[a + (b-a) \times e^{-e^{c}\times Time}\right]$. The detail of each variable was described in the materials and methods. Only significant coefficients (p-value <0.05) are shown for the three curves' fit. (For interpretation of the references to color in this figure legend, the reader is referred to the Web version of this article.)

Table 2
Guided Bone Regeneration Predictive Recovery Score applied to the study cohort.

	Guided Bone Regeneration Predictive Recovery Score			Total
	PR0 - Failure	PR1 - Follow-up	PR2 - Success	
Sex [Male|Female]				
p-value = 0.83				
CAS	10|11	-|-	14|4	39
ASM	3|2	-|-	18|19	42
ASMB	-|-	1|1	20|17	39
ASPBB	-|-	4|6	51|69	130
Group [n (%)]				
p-value<0.001				
CAS	21 (54)	0 (0)	18 (46)	39 (100)
ASM	5 (12)	0 (0)	37 (88)	42 (100)
ASMB	0 (0)	2 (5)	37 (95)	39 (100)
ASPBB	0 (0)	10 (8)	120 (92)	130 (100)
Age [Years±SD]				
Biomaterial p-value = 0.06,				
PR-score p-value = 0.08				
CAS	38 ± 14	- ± -	37 ± 10	37 ± 12
ASM	28 ± 9	- ± -	42 ± 15	40 ± 15
ASMB	- ± -	35 ± 7	43 ± 15	43 ± 15
ASPBB	- ± -	46 ± 18	47 ± 17	47 ± 17
Lesion at 6 months [%±SD]				
CAS	96.0 ± 3.0	- ± -	33.4 ± 6.1	67.1 ± 32.0
ASM	97.3 ± 0.8	- ± -	31.0 ± 6.4	38.8 ± 22.6
ASMB	- ± -	61.7 ± 9.7	18.3 ± 7.6	20.6 ± 12.3
ASPBB	- ± -	61.3 ± 7.2	12.5 ± 7.4	16.3 ± 15.0
Lesion curve parameters		a; b; c; d	a; b; c	–
CAS	99.82–0.61xT	–	97.1; 0.27; −1.71	–
ASM	99.82–0.61xT	–	98.3; −0.02; −1.61	–
ASMB	–	5.9; 2.6; 100; 6.9	94.8; 0.04; −1.12	–
ASPBB	–	−11.9; 1.9; 99.9; 8.4	96.6; 0.06; −1.43	

CAS: Conventional Apical Surgery; ASM: Apical Surgery with human fascia lata Membrane placement; ASMB: Apical Surgery human fascia lata Membrane placement and lyophilized allograft Bone powder; ASPBB: Apical Surgery with Porcine membrane and Bovine Bone; n: number of individuals; SD: Standard Deviation; %: perceptual value; "-": No data available for the variable and PR-score levels; T: Time in months; *a*, *b*, *c*, *d*: lesion curve parameters. Categorical variables were tested using a χ^2 test, with a simulated p-value for the group. Age was tested using a two-way Analysis of the Variance (ANOVA) for the study population and PR score, respectively. ANOVA assumptions for the lesion at six months were not satisfied. The lesion space is categorized into three scores —PR0 for failure, PR1 for follow-up, and PR2 for success. PR0 was modeled using linear decreasing growth; PR1 was modeled using an "S" shaped log-logistic curve $y = a + \frac{c-a}{1+e^{b\times[log\ (Time)\ -log\ (d)]}}$; PR2 was modeled using a "C" shaped cellular growth tendency $y = 100 - \left[a + (b-a) \times e^{-e^{c}\times Time}\right]$. The detail of each variable was described in the materials and methods. Only significant coefficients (p-value <0.05) are shown for the three curves' fit.

these patterns showed statistical differences based on the allograft material used ($p < 0.01$), indicating variations in population treatment response, as depicted by the three curves (blue for ASMB, green for ASM, and red for CAS) in Fig. 3a., where the ASMB had the fastest and earliest bone growth response, followed by ASM and CAS. No matter the material used, they all had a PV24 < 25 % (treatment success).

4.2. Biological interpretation of the time-evolution biomaterial-dependent patterns

The linear percentage lesion volume tendency can be expressed as 99.82 % – 0.61 % × Time. In addition, the random contribution showed that $\sigma_P^2 = 1.13 \times \sigma_\varepsilon^2$ and $\sigma_G^2 = 0.55 \times \sigma_\varepsilon^2$. Hence, the patient random deviation, σ_P^2, is just as big as the error counterpart, whereas the sex deviation, σ_G^2, is half of the random error σ_ε^2. This evidence is supported using linear mixed-effects models. On the contrary, the "S" shaped curve that can be modeled by a log-logistic regression and fitted by a non-linear least squares model, a+(c−a)/(1+exp{b × [log(Time)−log(d)]}) with parameters $a = 5.9$, $b = 2.6$, $c = 100$ and $d = 6.9$. Indeed, the higher asymptote $c = 100$ was the initial lesion, whereas the lower was $a = 5.9$, indicating a residual lesion. The halfway response between a and c was $d = 6.9$, with a decreasing slope of $b = 2.64$. This pattern shows a delay at the beginning of the osteocyte's growth, which departed its behavior from PR2 and rapidly recovered after 12 months. Finally, the "C" shaped cellular growth pattern 100−(a+(b−a) × exp{−exp[c] × Time}), which can be modeled using a nonlinear mixed-effects model with a similar coefficient interpretation.

4.3. Guided bone recovery characterization

Considering treatment success, the leading proportion (p) was a perfect success for ASMB (pASMB = 1.00, CI95 % [0.91; 1.00]), followed by ASM (pASM = 0.88, CI95 % [0.74; 0.96]) and CAS (pCAS = 0.46, CI95 % [0.30; 0.63]). This clearly demonstrated the association between treatment and outcome, as evidenced by the χ^2 test ($p < 0.001$, see Table 2). To further investigate treatment outcome proportion, posterior Marascuillo's test was applied to assess whether a significant difference exists (|pi−pj| with i≠j). The pCAS vs. pASM or pASMB differences were statistically significant in both cases with a $p < 0.001$. Regarding pASM vs. pASMB the absolute proportion difference is only |pASMB−pASM| = 0.12 with a marginal statistical tendency (p = 0.058).

4.4. Guided Bone Regeneration prognostic recovery score (PR score)

Further analysis of the bone neoformation in Fig. 3b (central panel), showed that the treatment outcome (PV24) could be explained by the bimodal density graph which splits the population into treatment success (purple dots) or failure (pink dots). Using a data-driven approach, we can consider the treatment success distribution with parameters μ = 2.30 % and $\boldsymbol{\sigma}$ = 2.09 % for the lesion volume %. Therefore, if we need to consider a treatment cut-off point for success, we can consider 10$\boldsymbol{\sigma}$ away the mean of this distribution, i.e., 2.30 % + 10 × 2.09 % = 23.20 % strictly speaking. However, the authors defined to use of 25 % as cut-off, which is an easy value to remember and confers an extra security margin. Then, the treatment outcome regions can be defined by the purple and pink rectangles (Fig. 3b).

Moving to the prognostic recovery score, the earliest time that correlates treatment outcome is PV6. Based on these findings, we developed a bioinformatics tool to objectively patient evaluation, using post-treatment images, which allow an early assessment of bone formation, to improve the current treatment success assessments that are usually determined at 12 or 24 months by CBCT, without inferring biomedical results or prognoses during that window, just as our main objective intended in the first place. Then, this evidence motivated us to define an early prognosis recovery score (PR score) using the PV6 membership to the two-population treatment success bell densities (success or failure). However, this concept undermined two patients, where 50 %<PV6<75 % (ivory area), and recovered the population pattern at 12 months, ending with a successful treatment at 24 months. Motivated by this evidence, the PR score can be formally defined into three categories (Fig. 3b).

- PR0: if PV6 > 75 %, i.e., treatment failure.
- PR1: if 75 % ≥ PV6 ≥ 50 %, i. e., surveillance at 12 months post-surgery.
- PR2: if PV6 < 50 % i. e., treatment success.

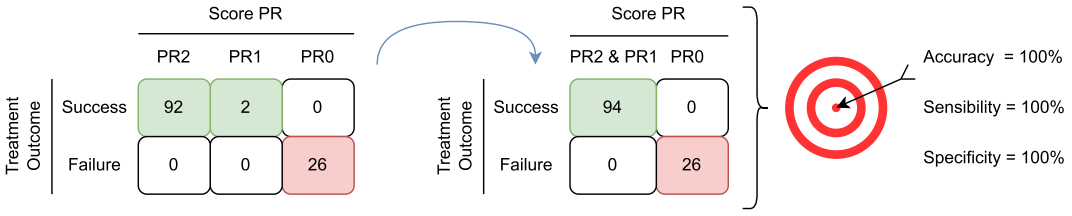

Fig. 4. Classification metrics. The score PR obtained at 6 months is contrasted against the treatment outcome at 24 months. The PR2 and PR1 scores are groped to create a 2-by-2 contingency table to assess the score PR classification metrics (accuracy, sensibility, and specificity).
PR: Prognostic Recovery. PR0-Failure, PR1-Follow-up, PR2-Success. Accuracy = (94 + 26)/120 × 100 %; Sensibility = 94/94 × 100 %; Specificity = 26/26 × 100 %.

Our PR score proposal was independent of the sex (P = 0.83), age (P = 0.06), or treatment (P = 0.08), using a χ^2 test (Table 2). Moreover, the three PR scores (PR0, PR1, and PR2) have shown three morphological behaviors as described before (linear, "S" or "C" shaped patterns). From a classification perspective, the treatment outcome (24 months) has two possible labels (success or failure) but, the PR score (6 months) has three (PR0, PR1, and PR2). However, the evidence of Fig. 3 has shown that PR1 and PR2 leads to treatment success whereas PR0 to failure. Hence, we can construct the confusion matrix of treatment outcome vs. PR score (Fig. 4) where we can group PR2 and PR1 into a single class to have a 2-by-2 contingency table where only the principal diagonal has non-zero values. This means that the proposed PR score hits the bullseye right in the center, i.e., a 100 % accuracy, sensitivity, and specificity (Fig. 4).

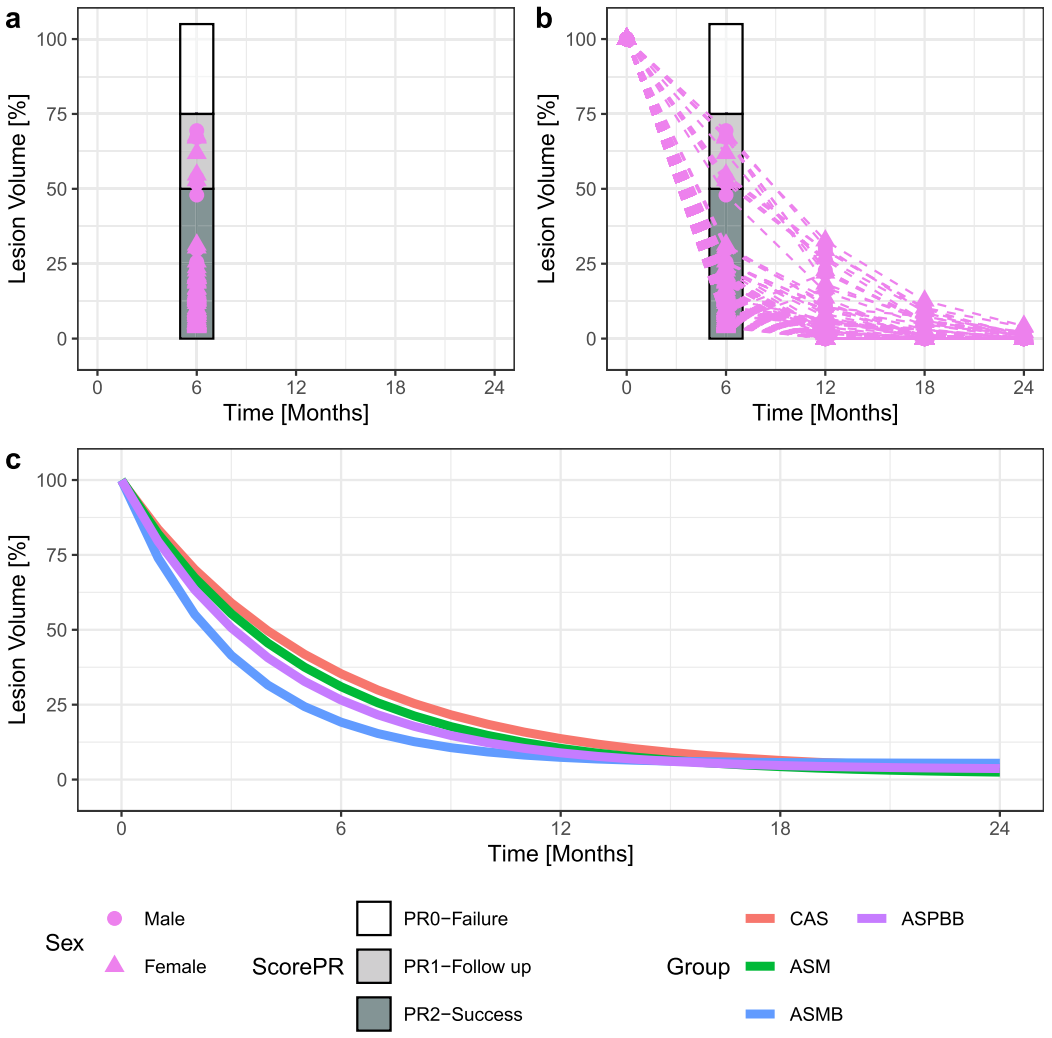

Fig. 5. Guided Bone Regeneration Predictive Recovery score (PR score) applied to bovine-porcine biomaterials. (a) The lesion volume time evolution outcome for Apical Surgery with Porcine membrane and Bovine Bone powder (ASPBB) at 6 months (in pink color) is used to assign one of the PR scores for PR0-Failure, PR1-Follow-up and PR2-Success according to the white, ivory, and gray filled rectangles, respectively. (b) The complete lesion volume time evolution for 0, 6, 12, 18, and 24 months (pink dots and dashed lines). Using this biomaterial, success was 100 % at 24 months, with PR0 of 0 % (0/130), PR1 of 8 % (10/130), and PR2 of 92 % (120/130). (c) Different biomaterial treatment behavior comparisons using PR score population "C" shaped the cellular growth tendency curve for the PR2 group. Different biomaterials were modeled from different angles, where treatment responders can be characterized by their recovery velocity in ASMB > ASPBB > ASM > CAS.
CAS: Conventional Apical Surgery; ASM: Apical Surgery with human fascia lata Membrane placement; ASMB: Apical Surgery human fascia lata Membrane placement and lyophilized allograft Bone powder; ASPBB: Apical Surgery with Porcine membrane and Bovine Bone. The "C" shaped cellular growth tendency $y = 100 - \left[a + (b-a) \times e^{-e^{c} \times Time}\right]$ where y was the observed percentage volume; a was the lower asymptote; b was the higher asymptote; c was the halfway response between a and b asymptotes. (For interpretation of the references to color in this figure legend, the reader is referred to the Web version of this article.)

4.5. External validation of PR score

The allograft cohort (CAS, ASM, and ASMB) with the xenograft cohort (ASPBB) did not present differences between the two graft materials regarding sex, age, and dental location (Tables 1 and 2). Fig. 5a showed for ASPBB that PR0 had 0 % patients (0/130), PR1 with 8 % (10/130), and PR2 with 92 % (120/130), which in terms of the treatment success represented pASPBB = 1.00, CI95 % (0.97; 1.00), (Fig. 5b). Moreover, a direct comparison of PR2 curves behavior (Fig. 5c and Table 2) showed that ASPBB had a different treatment recovery speed where ASMB > ASPBB > ASM > CAS from the fastest to the slowest. This objective biomaterial comparison on guided bone recovery time evolution can easily be applied to other allograft and xenograft material compositions.

5. Discussion

No literature has evaluated the Guided Bone Regeneration (GBR) response quantitatively and objectively. Through digital imaging and bioinformatic analysis of bone regeneration observed in Cone Beam Computed Tomography (CBCT), we designed a tool to measure the quantitative and objective assessment of the response of GBR to differentiate responders from non-responder patients and objectively compare the treatment efficacy. We defined three time-evolution curves depending on the biomaterials used in the GBR and we classified patients quantitatively, objectively, and precisely according to their biological response to these materials. Different morphological behavior was shown, i.e., a linear tendency, "S"-shaped log-logistics, or "C" cellular growth.

There has been controversy about whether the barrier membrane benefits include reducing bone resorption [17]. This work objectively and quantitatively confirmed that using the membrane in bone regeneration is essential to increase the effectiveness rate, with only 46 % (18/39) of success in the CAS group (without any membrane), compared with ASM patients (with only membrane) who showed a success rate of 88 % (37/42), and with the simultaneous use of membrane and lyophilized bone in the ASMB patients reached a success rate of 100 % (39/39), CI95 % (91; 100). In this study, we concluded that the best treatment is the one that uses both membrane and bone. Our findings concurred with Hardwich and colleagues, who reported clinical cases using absorbable membranes that showed a decrease in the failure rate and an increase in the speed of confirmation of the typical architecture of bone tissue [18]. Peterson and collaborators obtained similar results, including 2375 patients undergoing CAS, and 36 % resolved successfully after the intervention [19]. Our time-evolution curve biomaterial-dependent confirmed that the membrane speeds up the recovery time, and membrane treatments have a quantitative effectiveness rate of 100 percent for allograft and xenograft biomaterials. Low success rates in our study's "CAS" group might be associated with initial lesion size and consequent epithelial tissue growth into the surgical wound even before the bone tissue could recover.

Moreover, a direct comparison of the curves' behavior showed a different treatment recovery speed where ASMB > ASPBB > ASM > CAS from the fastest to the slowest. Bone formation takes longer with xenografts than with autogenous grafts, which might be explained by Oryan and Liu, who suggested that xenografts conserved both osteoinductive and osteoconductive characteristics but lacked the osteogenic properties of autografts [7,8]. Unfortunately, we have not been able to obtain all the patients' immunohistochemical staining results to support this Oryan suggestion. Oryan et al. also described that, depending on the origin, xenografts could carry a risk of transmission of zoonotic diseases; thus, graft rejection would be more likely and aggressive [8]. Nevertheless, our external validation using a bovine bone matrix implant and collagen membrane of porcine origin (ASPBB, n = 130) determined no such graft rejection, showing 100 % treatment success.

We also developed a bioinformatic tool to evaluate patients objectively using post-treatment images. This allows an early assessment of bone formation to improve the current treatment success assessments, usually determined at 12 or 24 months by CBCT. The GBR Predictive Recovery Score (PR score) used only two CBCT volume assessments (0 and 6 months), allowing us to compare the treatment efficacy objectively. Our study population, according to the PR score developed, was made up of the PR0 (failure) group with 26/250 (10 %) patients: 21/39 (54 %) with CAS, 5/42 (12 %) with ASM, 0/39 and 0/130 with ASMB and ASPBB respectively. In the PR1 group, 12/250 (5 %) patients: 0/39 CAS, 0/42 ASM, 2/39 (5 %) ASMB, and 10/130 (8 %) ASPBB. And finally, by the PR2 (success) group with 212/250 (85 %) patients: 18/39 (46 %) of CAS, 37/42 (88 %) of ASM and 37/39 (95 %) of ASMB, and 120/130 (92 %) of ASPBB. This analysis shows that the PR score is an excellent biomedical imaging tool to predict the outcome of apical microsurgery with GBR. This observation reinforces the PR scoring model approach since the PR0/1/2 classifications follow the curves of time evolution, linear tendency, and S and C-shaped curves, respectively. Then, the PR score could be used to determine the personalized response of bone regeneration through CBCT (PV0 and PV6) with different biomaterials, thus ensuring the success rate of apical microsurgery or implant therapy is independent of long-term regeneration and predicted patient response post-surgery. New bone formation requires CBCT evaluation at 24 months, which results in a loss of time for patients who need further treatment. The CBCT scans at 0, 6, 12, 18, and 24 months were only performed in the PR cohort to fully characterize the lesion recovery time evolution curve. However, CBCT every six months would be contraindicated in clinical practice mainly due to excessive exposure to radiation and the high cost that accurate monitoring adds to the health system, leading to an imprecise diagnosis of bone neoformation. The proposed PR-score strategy designed by Digital Bioinformatics only uses 0 and 6 months to assess the treatment success accurately. In this way, it is possible to differentiate earlier responders from non-responders, reducing the cost of imaging follow-up to a single extra CBCT at six months, given that presurgery CBCT is a reasonable practice requirement. In this way, radiation exposure is reduced to the minimum possible, and the imaging cost. We demonstrated this in the Validation cohort, where we have shown with high specificity and sensitivity that the extended response can be predicted with just a CBCT at six months using our PR score.

This study has limitations. We have not obtained immunohistochemical staining results for all patients to affirm that the lack of osteogenic properties correlates with the lack of eliminative antigenicity. However, we have obtained impressive results by obtaining a PR scoring strategy designed by Digital Bioinformatic that only uses 0 and 6-month CBCT to accurately evaluate the success of Apical Surgery-GBR with different biomaterials, which can be used whether allograft or xenograft.

6. Conclusions

Through digital imaging and bioinformatic analysis of bone regeneration observed in CBCTs, we defined three time-evolution curves depending on the biomaterials that confirm the membrane speeds up the recovery time. We also defined a GBR Prognostic Recovery Score (PR score) using only two CBCT volume assessments (0 and 6 months), allowing us to compare the treatment efficacy objectively. Then, patients' treatment outcomes can be predicted quantitatively, objectively, and precisely with this PR score, according to their biological response to allograft or xenograft materials (time-evolution bone growth curves). This score objectively classified post-surgery responders from non-responder patients, reducing follow-up costs and radiation exposure.

Ethics statement

The Ethics Commission of the Faculty of Dentistry of the University of Buenos Aires reviewed and approved this study (0016412/2011). All participants/patients (or their proxies/legal guardians) provided informed consent to participate in the studies and publication of their anonymized images.

Funding sources

This research was supported by the University of Buenos Aires (UBA).

Limitation statement

We have not been able to obtain the immunohistochemical staining results of all the patients to support this study, so we cannot affirm that the lack of osteogenic properties was correlated with no eliminating antigenicity.

Data availability statement

Data will be available upon request. Bioinformatic proposed PR score and lesion time evolution model used to fit this article data can be found at https://github.com/kachelo/scorePR.

Data statement

The data used and/or analyzed during the current study are contained within the manuscript or available from the corresponding author at a reasonable request. Available data models can be found at https://github.com/kachelo/scorePR.

CRediT authorship contribution statement

Pablo Rodríguez: Conceptualization, Project administration, Writing – original draft, Writing – review & editing. **Isabel Adler:** Conceptualization, Funding acquisition, Writing – review & editing. **María Lorena Cabirta:** Data curation, Writing – original draft, Writing – review & editing. **Eugenia Miklaszewski:** Data curation, Methodology, Writing – review & editing. **Nicolás Alfie:** Data curation, Methodology, Writing – review & editing. **Andrea Muiño:** Data curation, Methodology, Writing – review & editing. **Sara Chulián:** Data curation, Methodology, Writing – review & editing. **Cristóbal Fresno:** Formal analysis, Methodology, Software, Writing – original draft, Writing – review & editing. **Valeria Denninghoff:** Conceptualization, Supervision, Visualization, Writing – original draft, Writing – review & editing.

Declaration of competing interest

The authors declare that they have no known competing financial interests or personal relationships that could have appeared to influence the work reported in this paper.

Acknowledgments

The authors thank J.C. Elverdin, H.J. Alvarez Cantoni, J. Fernández Solari, L. Sierra, and L. Pinasco for contributing to this work.

References

[1] S. Taschieri, M. del Fabbro, T. Testori, M. Saita, R. Weinstein, Efficacy of guided tissue regeneration in the management of through-and-through lesions following surgical endodontics: a preliminary study, Int. J. Periodontics Restor. Dent. 28 (2008) 265–271.

[2] Y.K. Kim, J.K. Ku, Guided bone regeneration, J. Korean Assoc. Oral Maxillofac. Surg. 46 (2020) 361–366, https://doi.org/10.5125/jkaoms.2020.46.5.361.

[3] T. Kvist, C. Reit, The perceived benefit of endodontic retreatment, Int. Endod. J. 35 (2002) 359–365, https://doi.org/10.1046/j.1365-2591.2002.00486.x.

[4] P.A. Rodríguez, A.L. Lenarduzzi, L. Sierra, J. Fernández-Solari, J.C. Elverdin, Cirugía apical con utilización de membrana reabsorbible: Seguimiento a tres años de un caso clínico, Rev. Fac. Odontol. 25 (2010) 25–28.

[5] A. Oryan, S. Alidadi, A. Moshiri, N. Maffulli, Bone regenerative medicine: classic options, novel strategies, and future directions, J. Orthop. Surg. Res. 9 (2014) 1–27, https://doi.org/10.1186/1749-799x-9-18.

[6] A.H. Schmidt, Autologous bone graft: is it still the gold standard? Injury 52 (2021) S18–S22, https://doi.org/10.1016/j.injury.2021.01.043.

[7] J. Liu, D.G. Kerns, Mechanisms of guided bone regeneration: a review, Open Dent. J. 8 (2014) 56, https://doi.org/10.2174/1874210601408010056.

[8] A. Oryan, S. Alidadi, A. Moshiri, N. Maffulli, Bone regenerative medicine: classic options, novel strategies, and future directions, J. Orthop. Surg. Res. 9 (2014) 1–27, https://doi.org/10.1186/1749-799x-9-18.

[9] V.T. Athanasiou, D.J. Papachristou, A. Panagopoulos, A. Saridis, C.D. Scopa, P. Megas, Histological comparison of autograft, allograft-DBM, xenograft, and synthetic grafts in a trabecular bone defect: an experimental study in rabbits, Med. Sci. Mon. Int. Med. J. Exp. Clin. Res. 16 (2010) BR24–BR31.

[10] C.W. Cheah, N.M. Al-Namnam, M.N. Lau, G.S. Lim, R. Raman, P. Fairbairn, W.C. Ngeow, Synthetic material for bone, periodontal, and dental tissue regeneration: where are we now, and where are we heading next? Materials 14 (2021) 6123, https://doi.org/10.3390/ma14206123.

[11] G. Guess, A.M. Fouad, K. Meetu, B. Karabucak, S. Kratchman, in: En K. Syngcuk, S. Kratchman (Eds.), Cone Beam Computed Tomography, Microsurg, 2017, https://doi.org/10.1002/9781119412502.ch14. *Endod.*

[12] T. Schloss, D. Sonntag, M.R. Kohli, F.C. Setzer, A comparison of 2- and 3-dimensional healing assessment after endodontic surgery using cone-beam computed tomographic volumes or periapical radiographs, J. Endod. 43 (2017) 1072–1079, https://doi.org/10.1016/j.joen.2017.02.007.

[13] S. Kim, S. Kratchman, Modern endodontic surgery concepts and practice: a review, J. Endod. 32 (2006) 601–623, https://doi.org/10.1016/j.joen.2005.12.010.

[14] L. Sbordone, A. Barone, M. Di Genio, L. Ramaglia, Tetracycline fibres used to control bacterial infection during guided tissue regeneration (GTR), Minerva Stomatol. 49 (2000) 27–34.

[15] D. Bates, M. Mächler, B. Bolker, S. Walker, Fitting linear mixed-effects models using lme4, J. Stat. Software (2015), https://doi.org/10.48550/arXiv.1406.5823.

[16] J.C. Pinheiro, D.M. Bates, Mixed-Effects Models in S and S-PLUS, Springer, New York, 2000, https://doi.org/10.1007/b98882.

[17] I.A. Urban, H. Nagursky, J.L. Lozada, K. Nagy, Horizontal ridge augmentation with a collagen membrane and a combination of particulated autogenous bone and anorganic bovine bone-derived mineral: a prospective case series in 25 patients, Int. J. Periodontics Restor. Dent. 33 (2013) 299–307, https://doi.org/10.11607/prd.1407.

[18] R. Hardwick, B.K. Hayes, C. Flynn, Devices for dentoalveolar regeneration: an up-to-date literature review, J. Periodontol. 66 (1995) 495–505, https://doi.org/10.1902/jop.1995.66.6.495.

[19] J. Peterson, J.L. Gutmann, The outcome of endodontic resurgery: a systematic review, Int. Endod. J. 34 (2001) 169–175, https://doi.org/10.1046/j.1365-2591.2001.00375.x.